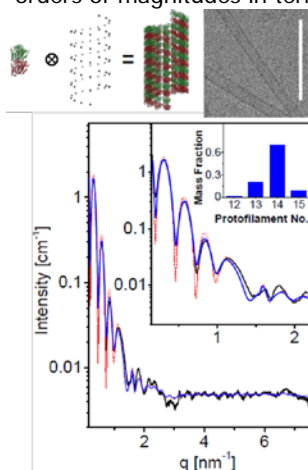


### Dynamics of tubulin nucleation and assembly

Tubulin assembles and disassembles into microtubule (MT) and multiple dynamic structures exhibiting complex behavior. MT assembly requires GTP-bound- $\alpha\beta$ -tubulin, and GTP hydrolysis by  $\beta$ -tubulin (into GDP) is required to generate dynamic MTs, operating out-of-equilibrium. Tubulin nucleation and MT assembly are highly abundant and important processes in cytoskeleton biology but poorly understood because the assembly is stochastic, occurs in solution, and involves GTP hydrolysis. Structural information at high spatial and temporal resolutions, in relevant solution conditions, is required to determine the underlying physics leading to the highly dynamic tubulin structures. Tubulin structures are often too dynamic, too soft, and too large in molecular weight to be crystalized. We have therefore used time-resolved solution X-ray scattering at ID02 beamline to study tubulin assemblies in solution. The scattering measurements were often supported by cryo-TEM, and a range of biophysical and biochemical methods. By applying **state-of-the-art data analysis, integrated with simulations, theory, and various algorithms, we have been studying the structures and intermolecular interactions in these complex, weakly ordered, and dynamic self-assembling structures. Our lab has developed the skills that are needed to study tubulin and MTs in their natural dynamic states.** We have developed our experimental protocols to purify tubulin<sup>1</sup> and study the high-resolution structure and dynamics of tubulin and MT<sup>1-2</sup> in their natural state (Figure 1) and in the presence of ions<sup>3</sup>.

In 2019 we have published our new **groundbreaking** software paper<sup>4</sup> for **solution X-ray scattering data analysis from large and complex macromolecular assemblies**. The program, called **D+**, is a comprehensive software, using our cutting edge state-of-the-art **algorithms**, containing more than *100,000 lines of open source C++ and CUDA codes*, running on both CPU and GPU platforms. The capabilities of **D+** exceeds earlier programs by several orders of magnitudes in terms of flexibility and complexity of the modeled structures, and computation speed (see Figure 7 in<sup>4-5</sup>). In **D+**, atomic or geometric models are docked into their assembly symmetry, describing how subunits repeat in a complex structure. This can be done in a hierarchical manner, in a bottom up approach, for many different subunits. In that way, **D+** can define any macromolecular assembly structure and compute its solution X-ray scattering curve at high resolution. **D+** has a **python wrapper**, which allows its integration with simulations, theory, and a range of advanced optimization and signal processing algorithms, enabling to attain unique dynamical and structural biophysical insight (see ref.<sup>1, 6-9</sup>).



**Figure 1.** Dynamic microtubule (MT) in the presence of GTP<sup>2, 4-5</sup>. Cryo-TEM image of MT (scale bar equals 200 nm)<sup>2</sup>. Solution X-ray scattering data (black curve) and models<sup>4-5</sup>. In the red model, the atomic tubulin model (PDB 3J6F) was docked into the three-start left-handed helical MT lattice (a radius of 11.9 nm, and a pitch of 12.214 nm), containing 14 protofilaments, as illustrated in the cartoon. In the blue model, the mass fraction distribution of protofilaments, shown at the smaller inset, was taken into account. Both models were computed by **D+**, and the hydration layer of the entire MT structure was taken into account<sup>4-5</sup>.

The nucleation of tubulin and its assembly into MT were studied in the presence of excess GTP. Assembly was triggered by a temperature jump from 5 to 37°C and followed by time-resolved X-ray scattering. The assembly reactions start from a solution of cold (5°C) tubulin and end in a solution of tubulin at 37°C. At the end point MTs form and Figure 1 demonstrates that the end point of the reaction is well characterized. We have also been focusing on determining the ensembles of structures and intermolecular interactions in cold GTP/GDP-tubulin solutions, under a wide range of conditions. We found that in cold tubulin solutions, tubulin dimers coexisted with tubulin oligomers and (GDP-rich) tubulin single rings. The concentration of solution strongly depends on the GTP and GDP concentrations. We have therefore investigated the assembly and disassembly conditions for single tubulin rings and their relation to the kinetics of MT assembly and disassembly. We determined the structure of tubulin single rings using cryo-TEM and solution X-ray scattering<sup>1</sup>. The scattering curves were fitted to models of tubulin single rings, constructed by docking the atomic model of the dimer (PDB 3J6F or 1SA0) into the ring symmetry and by taking the hydration layer of the ring into account, using **D+**, (Figure 2). We found that there is a critical concentration for ring formation. The critical concentration increased with GTP concentration or with temperature. We have also found that during MT assembly, the fraction of rings and unassembled tubulin dimers simultaneously decreased. During MT disassembly, however, the mass fraction of dimers increased but the increase in the concentration of rings was delayed until the fraction of dimers was sufficiently high and crossed the critical concentration for ring formation<sup>1</sup>.

To resolve the ensemble of GTP and GDP-tubulin assemblies formed at low temperature, we have used off-line size exclusion chromatography setup and analyzed the data of different fractions. We discovered that the solutions rapidly attained equilibrium (in the GDP-tubulin solution) or equilibrium-like state (in the GTP-tubulin solution). The entire SAXS data set were consistent with a thermodynamic model of tubulin single rings and curved tubulin oligomers. The analysis revealed a dimer-dimer association free energy of -14.2 and -13.2 k<sub>B</sub>T for GDP- and GTP-tubulin, respectively. Surprisingly, in the solution of GDP-tubulin, we have also detected a small fraction of stable tubulin single

rings, not predicted by the thermodynamic model. The radius of the rings was 19.2nm. In the GTP solution, the fraction of stable rings was significantly lower.

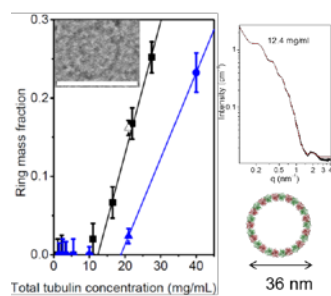


**Figure 2.** Mass fraction of tubulin in ring structures as a function of the total tubulin concentration. GDP-rich tubulin solutions before GTP was added (black) and after 4 mM GTP were added (blue). Cryo-TEM image of a tubulin ring is also shown (scale bar equals 50 nm)<sup>1</sup>. The measured scattering curve (black) and the fitted model (red) are shown on the right. The computed model is based on the atomic dimer structure (PDB 1SA0) which was docked into the symmetry of the ring (see cartoon at the bottom). In addition to the ring structure, the mass fraction of all the tubulin oligomeric ring fractions were taken into account. The mass fraction of all the tubulin assemblies was computed based on a thermodynamic model of macromolecular assemblies, based on which the dimer-dimer association free energy ( $-14.2$   $k_B T$  for GDP tubulin and  $-13.2$   $k_B T$  for GTP tubulin) was obtained by fitting the model to the scattering data. The paper describing the analysis is under preparation.

1. Shemesh, A.; Ginsburg, A.; Levi-Kalishman, Y.; Ringel, I.; Raviv, U., Structure, assembly, and disassembly of tubulin single rings. *Biochemistry* **2018**, *57* (43), 6153-6165.
2. Ginsburg, A.; Shemesh, A.; Millgram, A.; Dharan, R.; Levi-Kalishman, Y.; Ringel, I.; Raviv, U., Structure of dynamic, Taxol-stabilized, and GMPPCP-stabilized microtubule. *The Journal of Physical Chemistry B* **2017**, *121* (36), 8427-8436.
3. Raviv, D.; Asaf, S.; Abigail, M.; Yael, L.-K.; Israel, R.; Uri, R., *Hierarchical Assembly Pathways of Spermine Induced Tubulin Conical-Spiral Architectures*. 2020.
4. Ginsburg, A.; Ben-Nun, T.; Asor, R.; Shemesh, A.; Fink, L.; Tekoah, R.; Levartovsky, Y.; Khaykelson, D.; Dharan, R.; Fellig, A.; Raviv, U., D+: software for high-resolution hierarchical modeling of solution X-ray scattering from complex structures. *Journal of applied crystallography* **2019**, *52* (1), 219-242.
5. Ginsburg, A.; Ben-Nun, T.; Asor, R.; Shemesh, A.; Ringel, I.; Raviv, U., Reciprocal Grids: A Hierarchical Algorithm for Computing Solution X-ray Scattering Curves from Supramolecular Complexes at High Resolution. *Journal of Chemical Information and Modeling* **2016**, *56* (8), 1518-1527.
6. Asor, R.; Khaykelson, D.; Ben-nun-Shaul, O.; Oppenheim, A.; Raviv, U., Effect of Calcium Ions and Disulfide Bonds on Swelling of Virus Particles. *ACS omega* **2019**, *4* (1), 58-64.
7. Asor, R.; Selzer, L.; Schlicksup, C. J.; Zhao, Z.; Zlotnick, A.; Raviv, U., Assembly Reactions of Hepatitis B Capsid Protein into Capsid Nanoparticles Follow a Narrow Path Through a Complex Reaction Landscape. *ACS nano* **2019**.
8. Levartovsky, Y.; Shemesh, A.; Asor, R.; Raviv, U., Effect of Weakly Interacting Cosolutes on Lysozyme Conformations. *ACS Omega* **2018**, *3* (11), 16246-16252.
9. Louzon, D.; Ginsburg, A.; Schwenger, W.; Dvir, T.; Dogic, Z.; Raviv, U., Structure and intermolecular interactions between I-type straight flagellar filaments. *Biophysical journal* **2017**, *112* (10), 2184-2195.